PCP
PLANT & CELL PHYSIOLOGY

Regular Paper

Diminished Auxin Signaling Triggers Cellular Reprogramming by Inducing a Regeneration Factor in the Liverwort *Marchantia polymorpha*

Sakiko Ishida[1], Hidemasa Suzuki[1], Aya Iwaki[1,2], Shogo Kawamura[1], Shohei Yamaoka[1], Mikiko Kojima[3], Yumiko Takebayashi[3], Katsushi Yamaguchi[4], Shuji Shigenobu[4], Hitoshi Sakakibara[3,5], Takayuki Kohchi[1] and Ryuichi Nishihama[1,2,*]

[1]Graduate School of Biostudies, Kyoto University, Sakyo-ku, Kyoto, 606-8502 Japan
[2]Department of Applied Biological Science, Faculty of Science and Technology, Tokyo University of Science, Noda, Chiba, 278-8510 Japan
[3]RIKEN Center for Sustainable Resource Science, Tsurumi-ku, Yokohama, 230-0045 Japan
[4]Functional Genomics Facility, National Institute for Basic Biology, Okazaki, Aichi, 444-8585 Japan
[5]Graduate School of Bioagricultural Sciences, Nagoya University, Chikusa-ku, Nagoya, 464-8601 Japan

*Corresponding author: E-mail, nishihama@rs.tus.ac.jp
(Received 24 November 2021; Accepted 6 January 2022)

Regeneration in land plants is accompanied by the establishment of new stem cells, which often involves reactivation of the cell division potential in differentiated cells. The phytohormone auxin plays pivotal roles in this process. In bryophytes, regeneration is enhanced by the removal of the apex and repressed by exogenously applied auxin, which has long been proposed as a form of apical dominance. However, the molecular basis behind these observations remains unexplored. Here, we demonstrate that in the liverwort *Marchantia polymorpha*, the level of endogenous auxin is transiently decreased in the cut surface of decapitated explants, and identify by transcriptome analysis a key transcription factor gene, *LOW-AUXIN RESPONSIVE* (Mp*LAXR*), which is induced upon auxin reduction. Loss of Mp*LAXR* function resulted in delayed cell cycle reactivation, and transient expression of Mp*LAXR* was sufficient to overcome the inhibition of regeneration by exogenously applied auxin. Furthermore, ectopic expression of Mp*LAXR* caused cell proliferation in normally quiescent tissues. Together, these data indicate that decapitation causes a reduction of auxin level at the cut surface, where, in response, Mp*LAXR* is up-regulated to trigger cellular reprogramming. Mp*LAXR* is an ortholog of Arabidopsis *ENHANCER OF SHOOT REGENERATION 1/DORNRÖSCHEN*, which has dual functions as a shoot regeneration factor and a regulator of axillary meristem initiation, the latter of which requires a low auxin level. Thus, our findings provide insights into stem cell regulation as well as apical dominance establishment in land plants.

Keywords: AP2/ERF transcription factor • Apical dominance • Auxin • Cellular reprogramming • Liverwort *Marchantia polymorpha* • Plant regeneration

Introduction

Land plants display high plasticity during development and readily regenerate new tissues after being wounded or losing part of their body. In the early stage of regeneration, cellular reprogramming occurs to change the differentiation status of cells near a wound site, and the cell cycle is reactivated for cell proliferation (Umeda et al. 2021). In many cases, repeated cell divisions provide cell masses, or calli, which give rise to pluripotent stem cells that can direct morphogenesis of new organs or even whole plant bodies. In this process, plant hormones, such as auxin and cytokinin, regulate the change of cell fates.

Studies on tissue culture and grafting in angiosperms have revealed pivotal roles for auxin. During *de novo* root organogenesis from Arabidopsis cut leaf blades, YUCCA-mediated biosynthesis of auxin leads to its accumulation at the wound site, which promotes callus formation (Chen et al. 2016). Auxin signaling is also known to be involved in transcriptional regulation during root tip regeneration (Efroni et al. 2016). In the reunion process of incised inflorescence stems of Arabidopsis, endogenous auxin is polarly transported from the shoot apex and accumulates on the apical side but is depleted from the basal side, of the incision, which leads to side-specific cellular reprogramming responses for proper reunion (Asahina et al. 2011).

Analyses of molecular mechanisms for regeneration in Arabidopsis have revealed key transcription factors in the APETALA2/ETHYLENE RESPONSE FACTOR (AP2/ERF) family for cellular reprogramming. *WOUND INDUCED DEDIFFERENTIATION 1* (*WIND1*), encoding a class-I AP2/ERF, is rapidly induced in response to wounding and promotes callus formation (Iwase et al. 2011). WIND1 directly, and indirectly via

Plant Cell Physiol. 63(3): 384–400 (2022) doi:https://doi.org/10.1093/pcp/pcac004, Advance Access publication on 7 January 2022, available online at https://academic.oup.com/pcp

cytokinin, activates the expression of *ENHANCER OF SHOOT REGENERATION 1/DORNRÖSCHEN* (*ESR1/DRN*), a class-VIIIb AP2/ERF whose overexpression induces shoot regeneration in a cytokinin-independent manner (Banno et al. 2001, Iwase et al. 2017). In root regeneration, tissue damage induces the expression of class-X *ERF109* and *ERF115* via jasmonic acid signaling, which integrates auxin signaling for stem cell niche formation and tissue regeneration (Zhang et al. 2019, Zhou et al. 2019). In tissue reunion, class-X *ERF113/RELATED TO AP2 L* (*RAP2.6L*) is induced on the basal side of incised stems (Asahina et al. 2011). In the moss *Physcomitrium patens*, when a gametophore leaf is excised, cells near the cut site are reprogrammed directly into apical cells (Ishikawa et al. 2011). In this process, STEM CELL-INDUCING FACTOR 1 (STEMIN1), an AP2/ERF member of uncharacterized class, acts as a reprogramming factor (Ishikawa et al. 2019). These reports indicate that various types of AP2/ERF transcription factors are involved in regeneration in land plants.

Liverworts show a high capacity for regeneration, which does not require the application of any plant hormones (Kubota et al. 2013, Nishihama et al. 2015). When liverwort thalli are excised, new thalli regenerate from the ventral side of thallus explants (Vöchting 1885). In *Lunularia cruciata*, thallus regeneration requires the removal of the apical meristem, and slits or incisions on thalli are not as efficient in inducing regeneration; in addition, new thallus formation occurs only from apex-amputated (hereafter called 'basal') explants and not from any cut surfaces on apex-bearing (hereafter called 'apical') explants (Vöchting 1885, LaRue and Narayanaswami 1957). LaRue and Narayanaswami (1957) and later Rota and Maravolo (1975) demonstrated that exogenously applied auxin inhibits regeneration in *L. cruciata* and another liverwort species, *Marchantia polymorpha*, respectively. Therefore, thallus regeneration has been considered to be suppressed by apical dominance via apex-derived auxin. Consistent with this notion, auxin is transported basipetally in *M. polymorpha* (Gaal et al. 1982), and homologs of the major auxin biosynthesis pathway genes, *TRYPTOPHAN AMINOTRANSFERASE OF ARABIDOPSIS* (Mp*TAA*) and *YUCCA* (Mp*YUC2*), are expressed at the apex (Eklund et al. 2015). However, molecular mechanisms by which auxin controls thallus regeneration remain unexplored.

Previously, we reported cellular events and morphological changes in the early phase of regeneration in *M. polymorpha*. Apex amputation initiates a fate change of epidermal cells, and within 24 h, they re-enter the cell cycle and start to proliferate (Nishihama et al. 2015). In this study, using the model liverwort *M. polymorpha* (Kohchi et al. 2021), we aimed to uncover the roles of auxin in thallus regeneration and the mechanisms of cellular reprogramming toward cell cycle re-entry. By investigating changes in endogenous auxin levels and gene expression, we found that in basal explants, transient reduction of auxin levels triggered the expression of a key AP2/ERF transcription factor for cell cycle re-entry, providing a molecular basis for apical dominance.

Results

Repression of regeneration by auxin signaling in *M. polymorpha*

We first examined whether thallus regeneration in *M. polymorpha* is regulated by apical dominance in our culture conditions. Similar to the case for *L. cruciata* (Vöchting 1885, LaRue and Narayanaswami 1957), complete excision of the apex fully provoked regeneration in *M. polymorpha*, but a slit on the thallus was not as efficient as excision (**Supplementary Fig. S1**; Nishihama et al. 2015). We next examined the auxin-mediated inhibitory effect on thallus regeneration in *M. polymorpha* using different auxin compounds: indole-3-acetic acid (IAA), 1-naphthaleneacetic acid (NAA) and 2,4-dichlorophenoxyacetic acid (2,4-D). Ten-day-old wild-type thalli were bisected and basal fragments were further trimmed, generating rectangular explants, to investigate the polarity of regeneration (**Fig. 1A**). These explants were cultured on medium containing IAA, NAA or 2,4-D at various concentrations (**Supplementary Fig. S2**). Apical explants continued apical growth regardless of the presence of any auxin (**Fig. 1B** and **Supplementary Fig. S2**), indicating that auxin treatment at the concentrations examined did not exert detrimental effects on growth *per se*. Although basal explants formed several new buds from their apical side within 7 days when cultured without auxin, all auxin compounds inhibited regeneration from basal explants in a dose-dependent manner and, even if regeneration occurred, did not allow regeneration from any non-apical sides (**Fig. 1B** and **Supplementary Fig. S2**). Among them, NAA exerted the inhibitory effect on thallus regeneration at the lowest concentration (**Supplementary Fig. S2**). At the concentration of 1 μM, NAA inhibited regeneration in about 80% of basal explants, and only very small regeneration buds were formed on the other 20% (**Fig. 1C**). Hereafter, auxin treatment was conducted with NAA at 1 μM.

Auxin is perceived by TRANSPORT INHIBITOR RESPONSE 1/AUXIN SIGNALING F-BOX (TIR1/AFB)–AUXIN/INDOLE-3-ACETIC ACID (AUX/IAA) co-receptors and facilitates degradation of AUX/IAAs, which, in turn, enables AUXIN RESPONSE FACTOR (ARF) transcription factors to regulate the expression of their target genes (Weijers and Wagner 2016, Powers and Strader 2020). To examine whether the auxin-mediated transcriptional regulation is involved in the inhibition of regeneration, we analyzed the effect of a mutation in the sole activator-type *M. polymorpha* ARF Mp*ARF1*, which was reported to cause auxin insensitivity and developmental defects (Kato et al. 2017, 2020). We found that the basal explants of an Mp*arf1* knockout mutant (Kato et al. 2017) formed regeneration buds regardless of the presence of NAA (**Fig. 1D**). For further confirmation, we utilized a transgenic line expressing a domain-II-mutated, nondegradable version of the AUX/IAA (MpIAA^{mDII}) protein fused to a rat glucocorticoid receptor ligand-binding domain ($_{pro}$Mp*IAA*:Mp*IAA*^{mDII}-*GR*), where

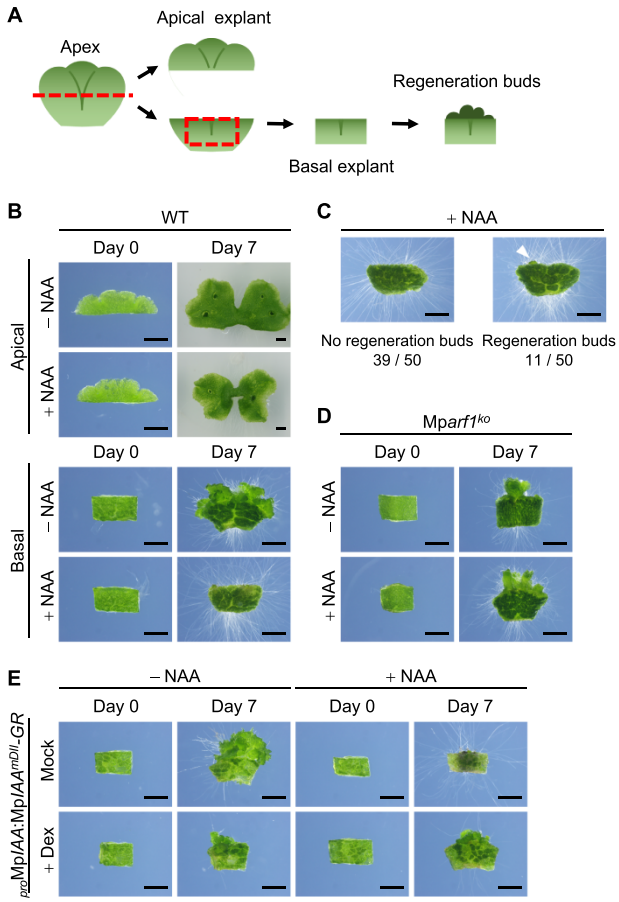

Fig. 1 Inhibition of thallus regeneration by exogenous auxin. (A) Schematic diagram for excision. A thallus lobe is divided into two pieces. The apex-containing half is used as an apical explant. The basal half is further excised as indicated and used as a basal explant. (B) Thallus regeneration in wild-type (WT) plants. Basal explants, prepared and placed as shown in A, were cultured with or without 1 μM NAA for 7 days. (C) Rates of regeneration bud formation from basal explants at day 7 in the presence of 1 μM NAA. Arrowhead indicates regeneration bud. (D) Regeneration assay, as in B, of the Mp*arf1-4*^{ko} mutant. (E) Regeneration assay under a dominant block of auxin signaling. Basal explants of $_{pro}$MpIAA:MpIAA^{mDII}-*GR* plants were cultured with or without 1 μM NAA in the presence or absence of 10 μM dexamethasone (Dex) for 7 days. Scale bars = 2 mm.

auxin signaling can be dominantly repressed upon treatment with dexamethasone (Dex) (Kato et al. 2015). Explants of $_{pro}$MpIAA:MpIAA^{mDII}-*GR* formed regeneration buds even on NAA-containing medium in a Dex-dependent manner (Fig. 1E), although the buds did not develop into thalli due to the effect of MpIAA^{mDII}, as shown previously (Kato et al. 2015). These results suggest that auxin signaling is involved in the suppression of regeneration.

Inhibitory effect of auxin on cell cycle re-entry during regeneration

Basal explants of *M. polymorpha* quickly reprogram quiescent ventral epidermal cells to re-enter the cell cycle by promoting the transition from G_1 to S phase to initiate the formation of regeneration buds (Nishihama et al. 2015). We examined whether auxin affects cell cycle re-entry by 5-ethynyl-2′-deoxyuridine (EdU) incorporation assay to visualize entry into S phase. Quantification of EdU-positive areas showed that cells that entered S phase greatly increased by 32 h after excision (HAE) in the absence of NAA (Fig. 2A-C), whereas in the presence of NAA, S-phase entry was barely observed even at 80 HAE (Fig. 2A, C). We further examined the expression level of Mp*CYCD;1*, a member of the D-type cyclins that have been shown to function in the activation of cell division in angiosperms and a moss (Masubelele et al. 2005, Ishikawa et al. 2011), by quantitative RT-PCR (qRT-PCR) in the narrow zone (~1 mm) near the cut surface in both apical and basal explants (Fig. 2D). Its transcripts significantly increased only in basal explants at 24 HAE. This up-regulation was suppressed, albeit not completely, in the presence of NAA (Fig. 2E), suggesting that the remaining Mp*CYCD;1* expression may not be sufficient to activate cell division. These results suggest that auxin exerts its inhibitory effect prior to cell cycle re-entry during regeneration.

Transient decrease in endogenous auxin level in basal explants

The inhibitory effect of auxin on regeneration implies differential changes in endogenous auxin levels between basal and apical explants. Quantification of indole-3-acetic acid (IAA) in the narrow cut surface (sampled as shown in Fig. 2D) revealed a sharp decrease of IAA levels in basal explants from 43.4 pmol/g fresh weight (gFW) to 14.5 pmol/gFW within 3 HAE and subsequent recovery to the original level by 24 HAE (Fig. 3A). By contrast, in apical explants, changes in IAA levels were mild with a gradual, smaller decrease to 21.2 pmol/gFW toward 12 HAE. These results suggest that the transient reduction of IAA level is involved in initiating regeneration.

To examine whether the changes in IAA levels in explants are correlated with auxin-responsive gene expression, we performed qRT-PCR for Mp*WIP*, an Mp*ARF1*-dependent, auxin-up-regulated gene (Kato et al. 2017). The expression level of Mp*WIP* was significantly reduced only in basal explants at 3 HAE and later recovered to some extent (Fig. 3B). In addition, NAA treatment up-regulated Mp*WIP* expression in both apical and basal explants (Fig. 3B). These data not only reinforce the observation of the drastic IAA reduction in basal explants but also suggest that the transient reduction of IAA level causes the down-regulation of auxin-up-regulated genes in basal explants.

Time-course transcriptome analysis during regeneration

To investigate transcriptional dynamics in response to excision, we performed RNA-seq analysis using apical and basal cut surface samples at various times up to 24 HAE. Principal component analysis (PCA) revealed differential transcriptional responses between apical and basal samples already at 1 HAE

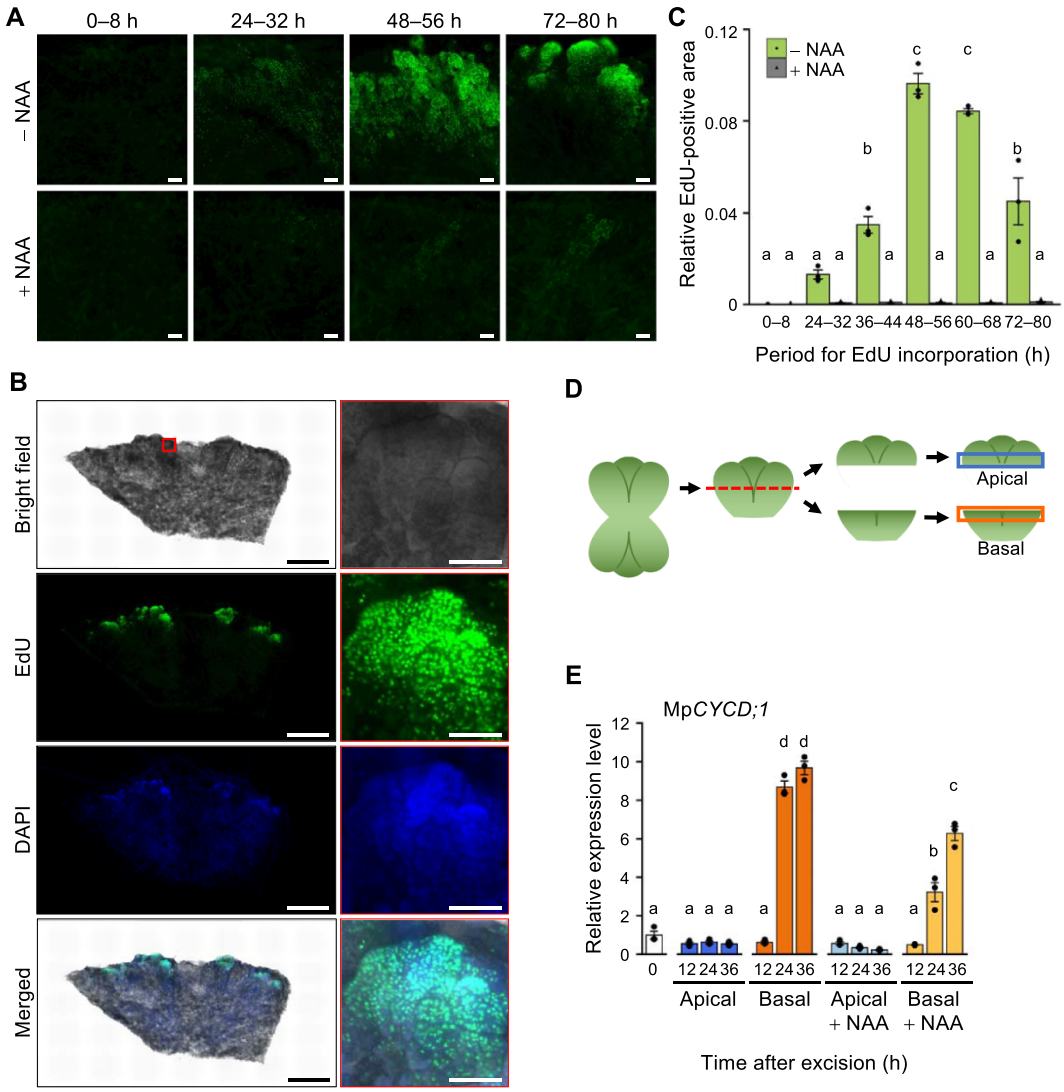

Fig. 2 Inhibitory effect of auxin on cell cycle re-entry during regeneration. (A, B) EdU incorporation assay to visualize S-phase progression in basal explants cultured with or without 1 μM NAA for the indicated time periods after excision. EdU-incorporated nuclei on the apical-side ventral surface around the midrib (A) and on the whole ventral surface of an explant at 80 HAE (B) were visualized with Alexa Fluor 488 (pseudo-colored in green). In B, all DNAs were stained with DAPI (pseudo-colored in blue), and magnified images for the area in the red box are shown in the right panels. Scale bars = 100 μm (A, B right panels), 1 mm (B left panels). (C) Quantification of EdU-positive areas in the experiments shown in A. EdU-positive area was quantified relative to the whole explant area, as described in Methods. Bars represent mean ± SE from three independent experiments. Letters above the bars indicate grouping by *P*-value < 0.05 in a Tukey–Kramer test. $n = 3$. (D) Experimental scheme for the quantification of gene expression and plant hormones. A thallus lobe was bisected and, after incubation, 1-mm sections (blue and orange boxed areas) were excised from the original cut surface of the apical and basal fragments. (E) Relative expression levels of Mp*CYCD;1* determined by qRT-PCR in apical and basal explants (sampled as shown in D) cultured with or without 1 μM NAA for the indicated times (in hours) after excision. Mp*EF1* was used for normalization. Bars represent mean ± SE from three biologically independent experiments. Symbols above the bars indicate grouping by *P*-value < 0.05 in a Tukey–Kramer test.

(**Fig. 4A**). Clustering and gene ontology (GO) enrichment analyses identified four clusters (C1–C4) of genes with distinct expression patterns and functions (**Fig. 4B, C**; **Supplementary Fig. S3**). C1 contained 1,801 genes that were up-regulated only in basal explants during the time course and that are involved in cellular activities, such as translation and cell division; C2 contained 877 genes that were up-regulated immediately after excision in both apical and basal samples and that are related to stress responses; C3 contained 1,281 genes that were down-regulated in both samples but more drastically in basal explants and that are associated with photosynthesis; C4 contained 224 genes that were slightly up- and down-regulated in apical and basal samples, respectively, but were not enriched in any GO terms.

We also performed RNA-seq analysis using NAA-treated basal samples to examine the influence of auxin on

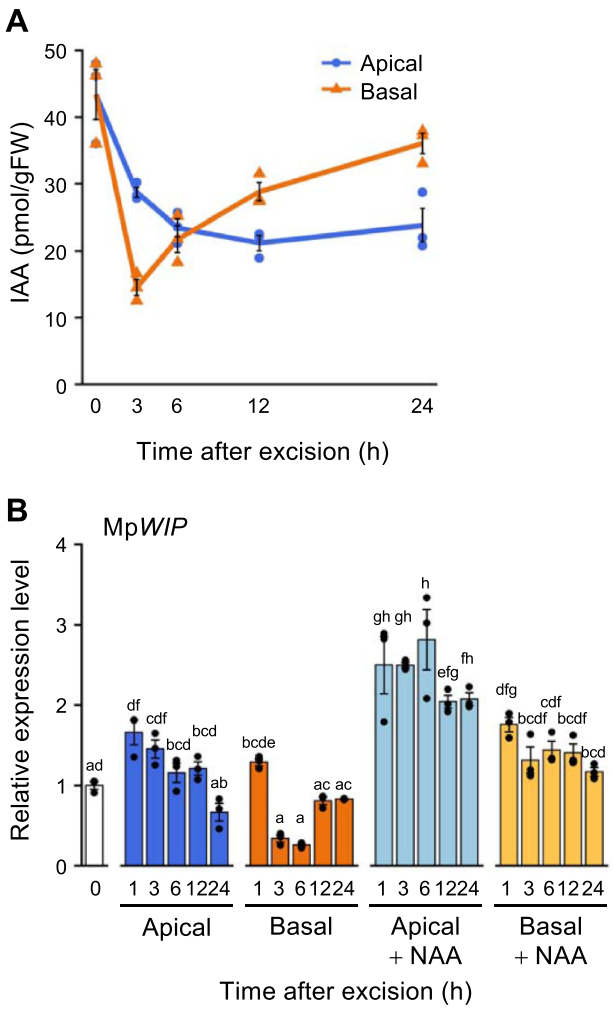

Fig. 3 Transient reduction of the endogenous auxin level in basal explants. (A) Quantification of the levels of IAA in the cut surface of apical and basal explants sampled as shown in **Fig. 2D**. Bars represent mean ± SE from three biologically independent experiments. (B) Relative expression levels of Mp*WIP* determined by qRT-PCR in the cut surface of apical and basal explants (sampled as shown in **Fig. 2D**) cultured with or without 1 μM NAA for the indicated times (in hours) after excision. Mp*EF1* was used for normalization. Bars represent mean ± SE from three biologically independent experiments. Letters above the bars indicate grouping by *P*-value < 0.05 in a Tukey–Kramer test.

transcriptional changes. PCA suggested transcriptomic profile changes by NAA treatment at 6 HAE (**Fig. 4A**). Fisher's exact test revealed a tendency for down-regulation of auxin-regulated genes in basal explants (**Fig. 4D**), which is consistent with the above-mentioned result of Mp*WIP* down-regulation in basal explants (**Fig. 3B**). These data suggest that differential expression of auxin-regulated genes contributes to distinct regeneration capacities between apical and basal explants.

Identification of Mp*LAXR* as a low-auxin-responsive transcription factor gene in basal explants

To identify key cellular reprogramming factors that trigger cell cycle re-entry, we examined genes in C1 that were up-regulated only in basal explants and those that were down-regulated by NAA treatment at 3 HAE. Among 29 genes that met both criteria (**Fig. 5A**; **Supplementary Table S1**), we focused on Mp*ERF20*, the only gene that was predicted to encode a transcription factor, which belongs to class VIIIb of the AP2/ERF family (Bowman et al. 2017, Chandler 2018). qRT-PCR analysis showed that Mp*ERF20* was up-regulated only in basal explants and that this induction was significantly, albeit incompletely, inhibited by NAA treatment (**Fig. 5B**).

If Mp*ERF20* is important for regeneration, it is conceivable that its expression would be promoted in response to auxin reduction. To test this possibility, without being influenced by wounding, intact gemmalings were treated with the auxin biosynthesis inhibitors 4-phenoxyphenylboronic acid (PPBo) (Kakei et al. 2015), yucasin (Nishimura et al. 2014) or L-kynurenine (He et al. 2011), and Mp*ERF20* expression levels were examined. qRT-PCR analysis revealed that the treatment with the auxin biosynthesis inhibitors indeed induced Mp*ERF20* expression (**Fig. 5C**). In addition, suppression of auxin signaling by Dex treatment of $_{pro}$Mp*IAA*:Mp*IAA*^{mDII}-*GR* plants also induced Mp*ERF20* expression (**Fig. 5D**). These results demonstrate that Mp*ERF20* is responsive to reduced auxin signaling, and Mp*ERF20* was renamed *LOW-AUXIN RESPONSIVE* (Mp*LAXR*).

To examine the spatiotemporal pattern of Mp*LAXR* induction during regeneration, we generated reporter lines expressing a fluorescent protein, tdTomato, fused to a nuclear localization signal (NLS) under the Mp*LAXR* promoter ($_{pro}$Mp*LAXR:tdTomato-NLS*). Right after excision of thalli of these reporter lines, no detectable fluorescent signal was observed on the ventral cut surface of basal explants (**Fig. 5E**, 0 h). Continued observation demonstrated that fluorescent signals became faintly detectable along the midrib preferentially on the apical side at 12 HAE and intensified at 24 HAE, by which time signals were also detected in the periphery of the midrib (**Fig. 5E**). However, in the presence of NAA, such signals were hardly detected (**Fig. 5E**). These results suggest excision-induced, auxin-repressive expression of Mp*LAXR* in cells on or near the midrib of basal explants, consistent with the previously reported preference for regeneration bud formation from the midrib region (Vöchting 1885, Nishihama et al. 2015).

Delay in cell cycle re-entry in Mp*laxr* mutants during regeneration

We further investigated whether the function of Mp*LAXR* is required for regeneration. Two alleles of Mp*laxr* mutants generated by CRISPR/Cas9 (**Supplementary Fig. S4**) exhibited only a slight growth defect, which was complemented, albeit partially, by introducing an Mp*LAXR* genomic fragment with synonymous CRISPR-resistant mutations (*gMpLAXRresist*; **Fig. 6A, B**). In contrast, severe retardation of regeneration bud growth was observed in the absence of Mp*LAXR*, and was fully rescued by the complementation cassette (**Fig. 6C, D**). The observed differences in complementation degrees between the two processes may reflect those in Mp*LAXR* expression levels required for

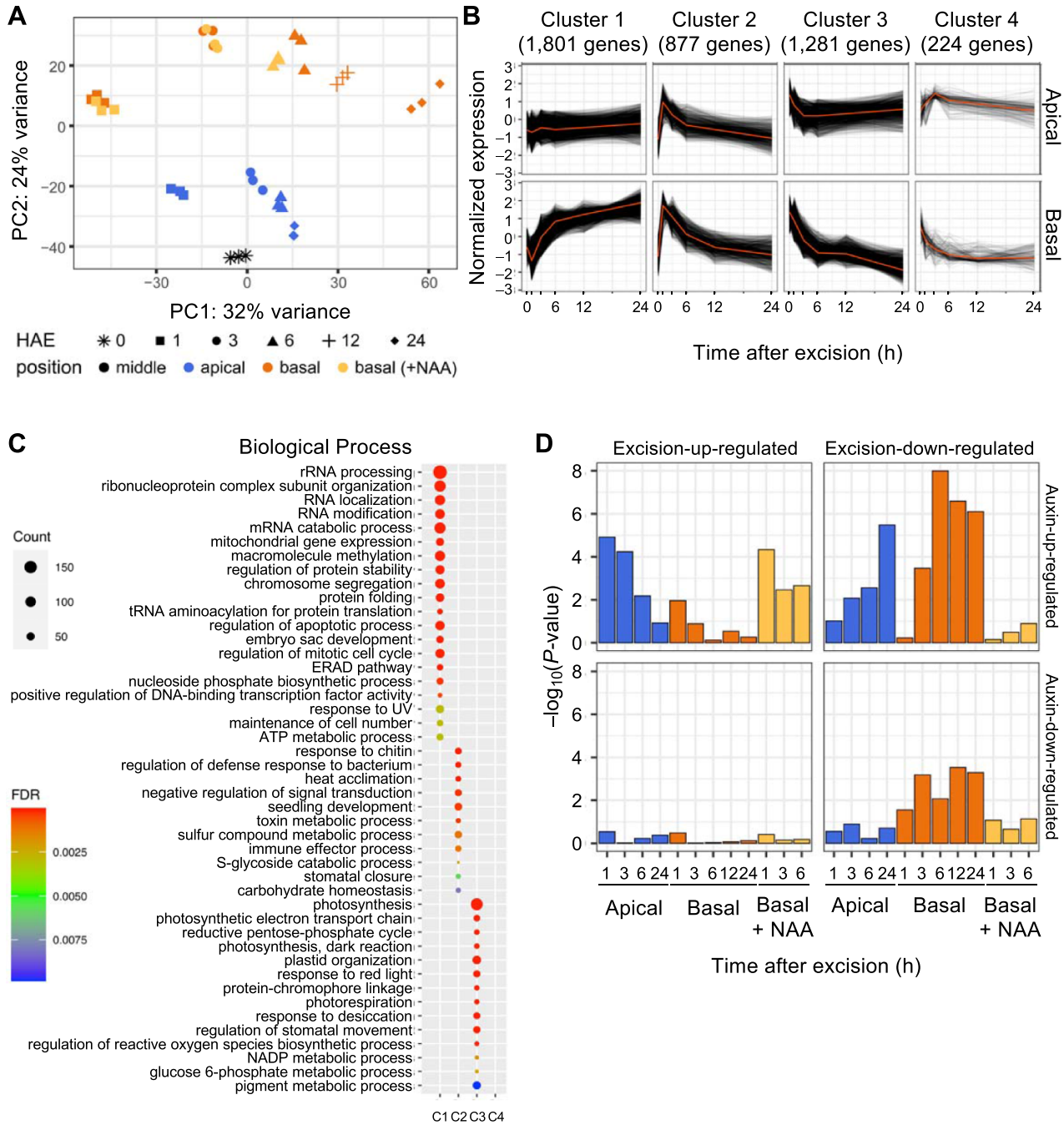

Fig. 4 Time-course transcriptome analysis during regeneration. (A) Principal component analysis of RNA-seq data. PCA was used to visualize the overall effects of explant position, time (hours) after excision (HAE), and exogenous auxin treatment on gene expression profiles. The first and second principal component values (PC1 and PC2, respectively) of each sample are plotted. (B) Clustering analysis using apical and basal time-course RNA-seq data. (C) GO enrichment analysis. Representative enriched GO terms in 'Biological Process' are listed in the order of false discovery rate (FDR; color-coded). Circle size represents the number of genes found in each cluster (C1–C4). (D) Tendency for down-regulation of auxin-regulated genes in basal explants. Fisher's exact test was used to evaluate the enrichment of auxin-up- or -down-regulated genes in excision-up- or -down-regulated genes at each time point (in hours) compared with time 0. *P*-values are shown. Genes up- or down-regulated by 1 h treatment of thallus with 2,4-dichlorophenoxyacetic acid (2,4-D), reported by Mutte et al. (2018), were used as auxin-regulated genes.

each process. EdU assay revealed substantial delays in cell cycle re-entry after excision for Mp*laxr* explants (**Fig. 7A, B**). Furthermore, induction of Mp*CYCD;1* expression in basal explants of Mp*laxr* mutants was significantly weaker than that of wild type (**Fig. 7C**). Taking these results together, Mp*laxr* mutations affected an early step of regeneration, similar to the outcome

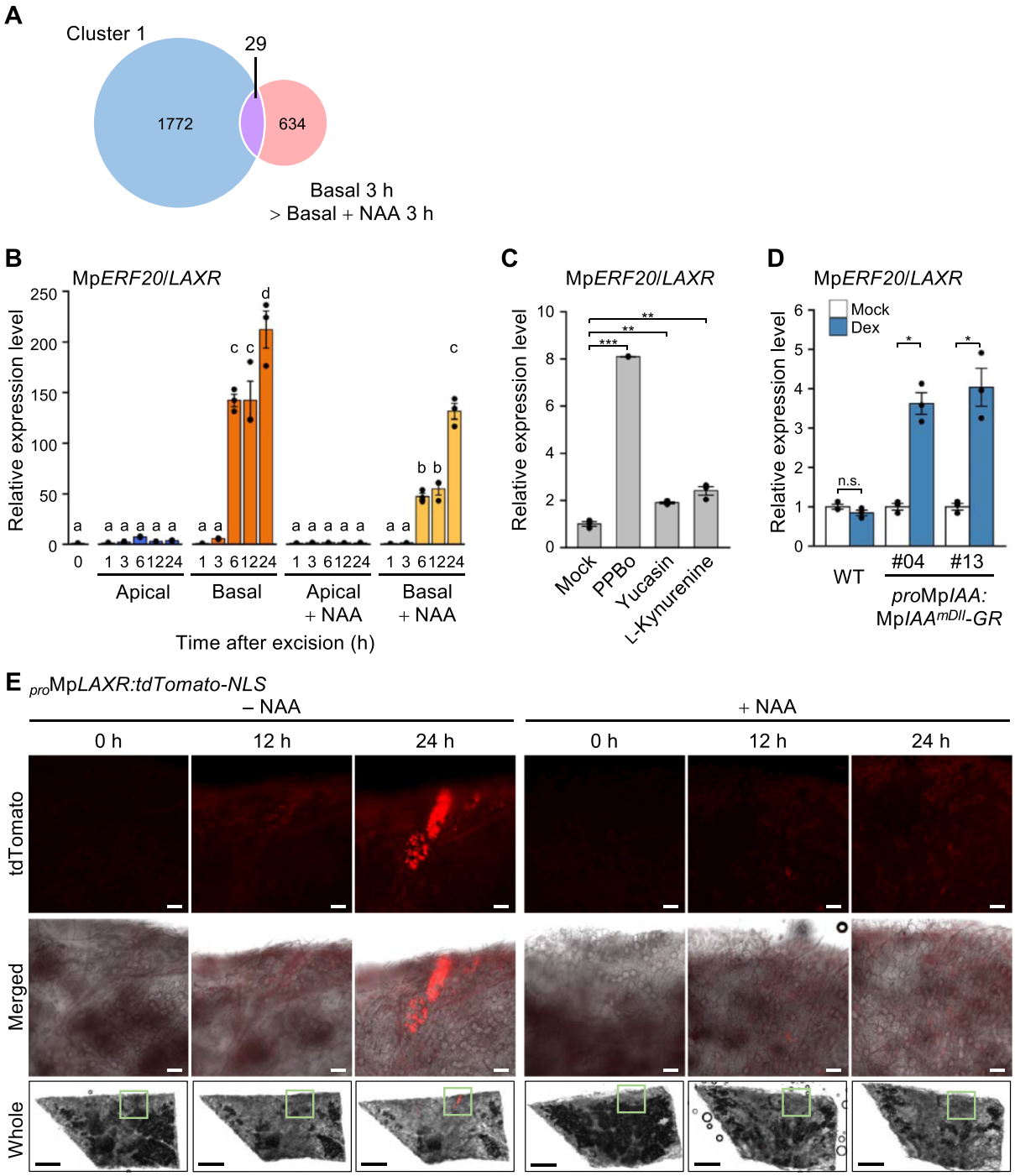

Fig. 5 Identification of Mp*LAXR* as a transcription factor up-regulated by decapitation. (A) Venn diagram comparing genes in cluster 1 and those down-regulated by NAA treatment for 3 h. (B) Relative expression levels of Mp*ERF20* (now renamed Mp*LAXR*) determined by qRT-PCR in the cut surface of apical and basal explants (sampled as shown in **Fig. 2D**) cultured with or without 1 μM NAA for the indicated times (in hours) after excision. Mp*EF1* was used for normalization. Bars represent mean ± SE from three biologically independent experiments. Letters above the bars indicate grouping by *P*-value < 0.05 in a Tukey–Kramer test. (C) Relative expression levels of Mp*LAXR* in gemmalings treated with or without auxin biosynthesis inhibitors (10 μM PPBo, 10 μM yucasin and 100 μM L-kynurenine) for 3 days. Asterisks (** and ***) indicate significant differences compared with mock treatment at $P < 0.01$ and $P < 0.001$, respectively, determined by Welch's two-tailed paired *t*-tests. (D) Relative expression levels of Mp*LAXR* in 10-day-old WT and *pro*Mp*IAA:*Mp*IAA*^{mDII}*-GR* plants (lines 4 and 13) with or without Dex treatment. Asterisks (*) indicate significant differences compared with mock treatment at $P < 0.05$ determined by Welch's two-tailed paired *t*-tests. n.s., not significant. (E) Time-lapse imaging of *pro*Mp*LAXR:tdTomato-NLS* basal explants treated with or without 1 μM NAA. Magnified images for tdTomato fluorescence without (top) or with merge on bright field images (middle) are shown for the green-boxed regions in the whole explant images (bottom; merged images are shown). Scale bars = 100 μm (top, middle), 1 mm (bottom). Similar results were obtained in other experiments.

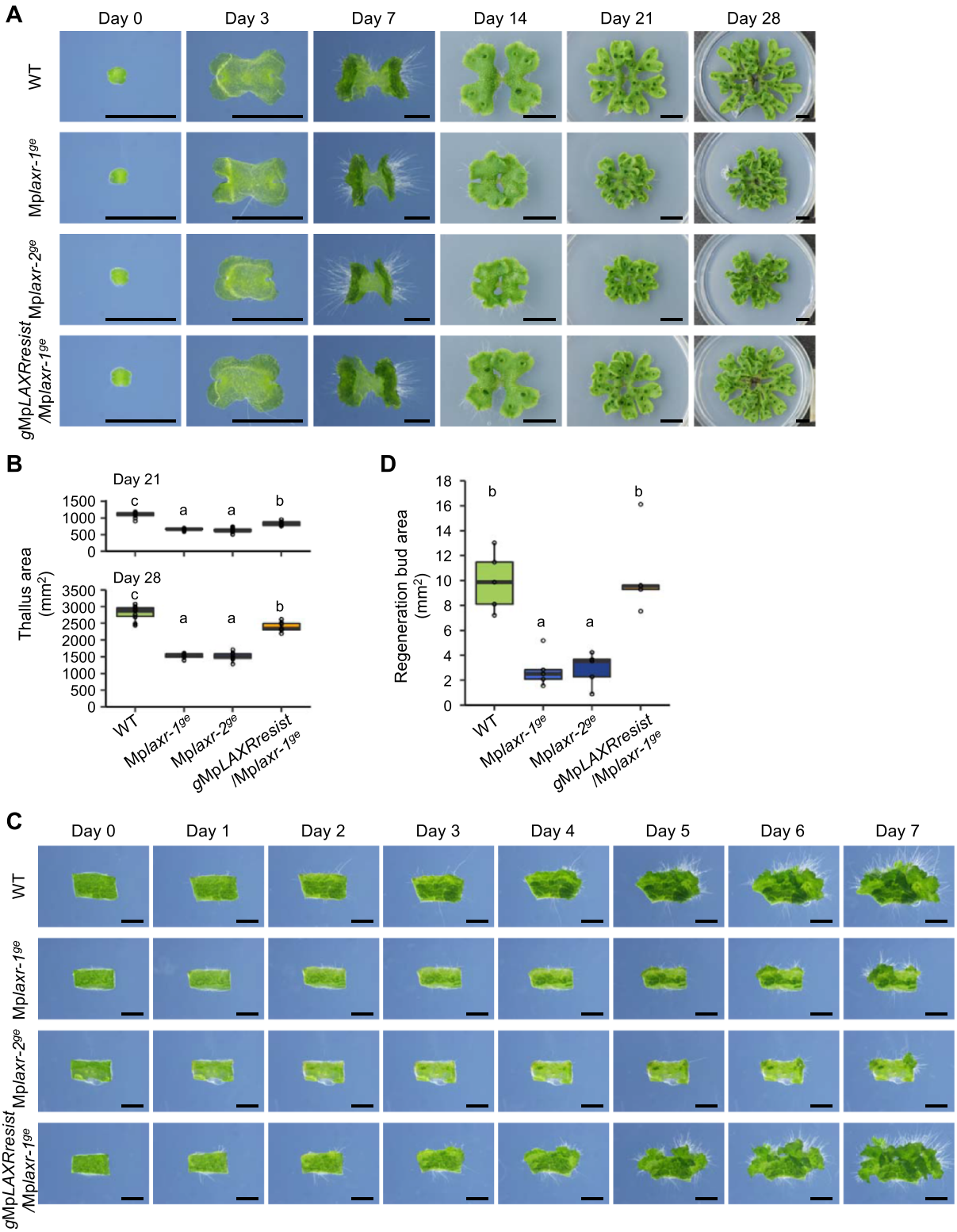

Fig. 6 Requirement of Mp*LAXR* for regeneration. (A) Growth of Mp*laxr* mutants. WT, Mp*laxr-1*^{ge}, Mp*laxr-2*^{ge} and *g*Mp*LAXRresist*/Mp*laxr-1*^{ge} gemmae were grown for 28 days. Scale bars = 2 mm (day 0–7), 10 mm (day 14–28). (B) Quantification of thallus areas of 21- and 28-day-old wild-type (WT), Mp*laxr-1*^{ge}, Mp*laxr-2*^{ge} and *g*Mp*LAXRresist*/Mp*laxr-1*^{ge} plants. Symbols above the bars indicate grouping by *P*-value < 0.05 in a Tukey–Kramer test. $n = 10$. (C) Time-course observation of WT, Mp*laxr-1*^{ge}, Mp*laxr-2*^{ge} and *g*Mp*LAXRresist*/Mp*laxr-1*^{ge} basal explants. Scale bars = 2 mm. (D) Quantification of areas of regeneration buds formed on WT, Mp*laxr-1*^{ge}, Mp*laxr-2*^{ge} and *g*Mp*LAXRresist*/Mp*laxr-1*^{ge} basal explants at 7 days after excision. Symbols above the bars indicate grouping by *P*-value < 0.05 in a Tukey–Kramer test. $n = 5$.

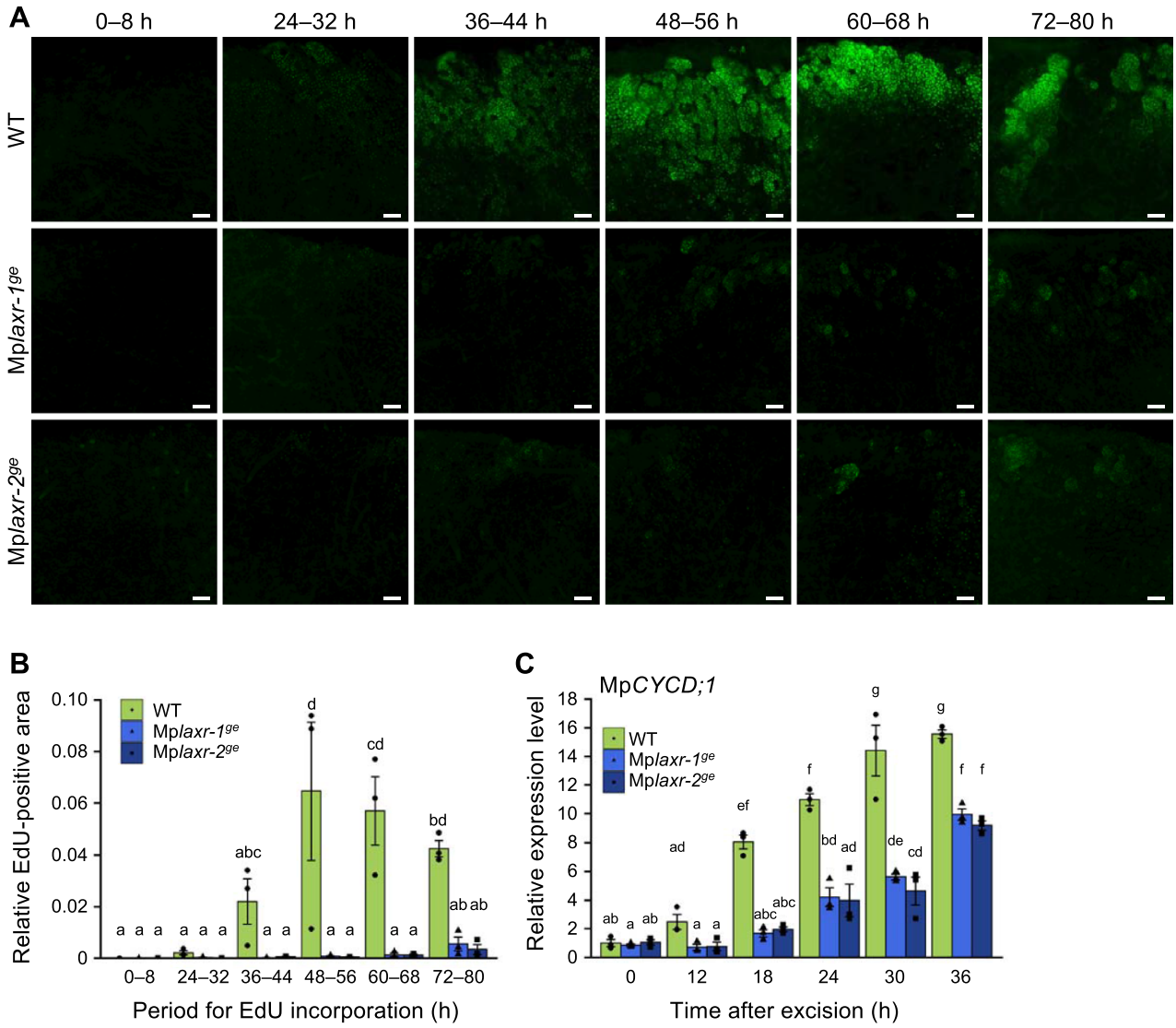

Fig. 7 Requirement of Mp*LAXR* for cell cycle re-entry toward regeneration. (A, B) EdU incorporation assay to visualize S-phase entry in basal explants of WT, Mp*laxr-1*^{ge} and Mp*laxr-2*^{ge} plants cultured for the indicated time periods after excision. EdU-incorporated nuclei on the apical-side ventral surface around the midrib were visualized with Alexa Fluor 488 (A) and quantified as EdU-positive area relative to the whole explant area, as described in Methods (B). Scale bars = 100 μm (A). Bars in B represent mean ± SE from three independent experiments. Letters above the bars indicate grouping by *P*-value < 0.05 in a Tukey–Kramer test. $n = 3$. (C) Relative expression levels of Mp*CYCD;1* determined by qRT-PCR in the cut surface of basal explants of WT and Mp*laxr* mutants (sampled as shown in **Fig. 2D**) at the indicated times after excision. Mp*EF1* was used for normalization. Bars represent mean ± SE from three biologically independent experiments. Symbols above the bars indicate grouping by *P*-value < 0.05 in a Tukey–Kramer test.

after auxin treatment. These results suggest that Mp*LAXR* plays a pivotal role in initiating regeneration.

Mp*LAXR* functions as a cellular reprogramming factor

Next, we examined whether the auxin-mediated inhibition of regeneration could be overridden by transient expression of Mp*LAXR* at the time of excision. To this end, we generated inducible Mp*LAXR* overexpressor lines using an estrogen receptor-based XVE transactivation system under the control of the *M. polymorpha E2F* promoter ($_{pro}$Mp*E2F:XVE*≫Mp*LAXR*; **Fig. 8A**). Estrogen-pre-treated thalli were cut, and explants were cultured in the presence or absence of NAA on estrogen-free medium. In wild type, NAA application inhibited regeneration regardless of estrogen pre-treatment (**Fig. 8B**), and similar results were obtained for estrogen-untreated $_{pro}$Mp*E2F:XVE*≫Mp*LAXR* explants (**Fig. 8C**). By contrast, estrogen-pre-treated $_{pro}$Mp*E2F:XVE*≫Mp*LAXR* explants formed new buds even in the presence of NAA (**Fig. 8C**). In addition, continuous estrogen treatment from the beginning of explant incubation with NAA also provoked cell division but did

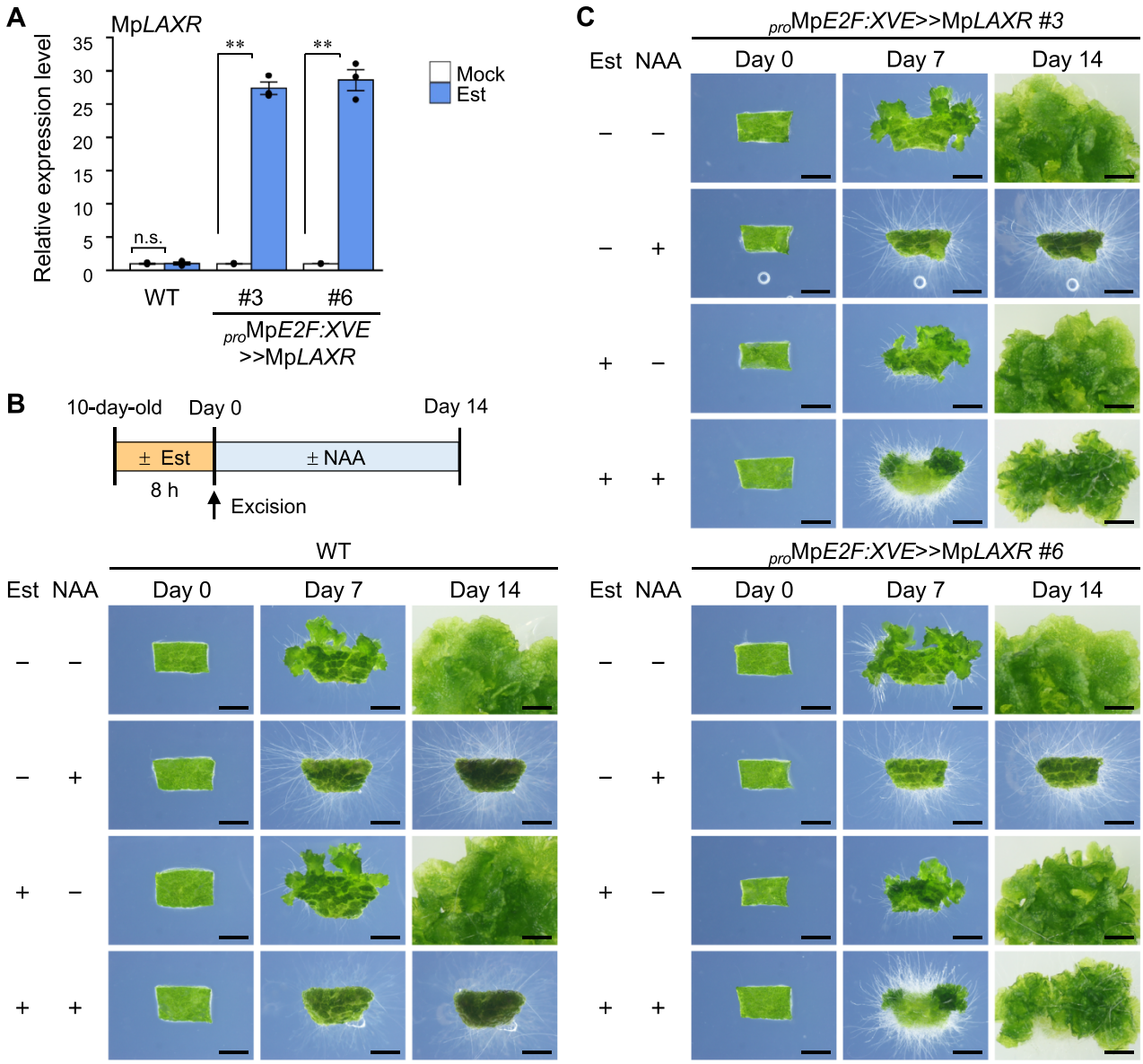

Fig. 8 Mp*LAXR* overexpression is sufficient for overriding regeneration suppression by auxin. (A) Relative expression levels of Mp*LAXR* determined by qRT-PCR in WT and $_{pro}$Mp*E2F:XVE*≫Mp*LAXR* plants (lines 3 and 6) cultured with or without 5 μM β-estradiol (Est) for 14 days. Mp*EF1* was used for normalization. Bars represent mean ± SE from three biologically independent experiments. Asterisks above the bars indicate a significant difference from mock for each line at $P < 0.01$ in a Welch's *t*-test. n.s., not significant. (B, C) Regeneration assay after transient expression of Mp*LAXR*. The reagent treatment is shown schematically at the top in B. Ten-day-old WT (B) and $_{pro}$Mp*E2F:XVE*≫Mp*LAXR* plants (C) were pre-treated with or without 5 μM Est for 8 h and then excised, and basal explants were cultured in the presence or absence of 1 μM NAA for 14 days. Scale bars = 2 mm.

not allow thallus development due to constant overexpression of Mp*LAXR* (**Supplementary Fig. S5**; see below). These results suggest that Mp*LAXR* nullifies the effect of NAA.

To explore the possibility of Mp*LAXR* being a cellular reprogramming factor, we examined whether Mp*LAXR* overexpression could induce cell division in normally quiescent cells. While $_{pro}$Mp*E2F:XVE*≫Mp*LAXR* gemmae developed into thalli with no apparent developmental defects in the absence of estrogen (**Fig. 9A**), estrogen treatment caused the formation of cell masses from not only the meristematic region but also the gemma periphery (**Fig. 9A, B**), whose cells do not divide during normal development, as revealed by EdU assay (**Fig. 9C**). Peripheral cells may be more sensitive for reprogramming, or the Mp*E2F* promoter more active in those cells, although further studies will be required to explain this observation. Scanning electron microscopy revealed that Mp*LAXR*-induced cell masses contained apparently undifferentiated small cells and rhizoids (**Fig. 9B, D** + Est). The small cells resembled those

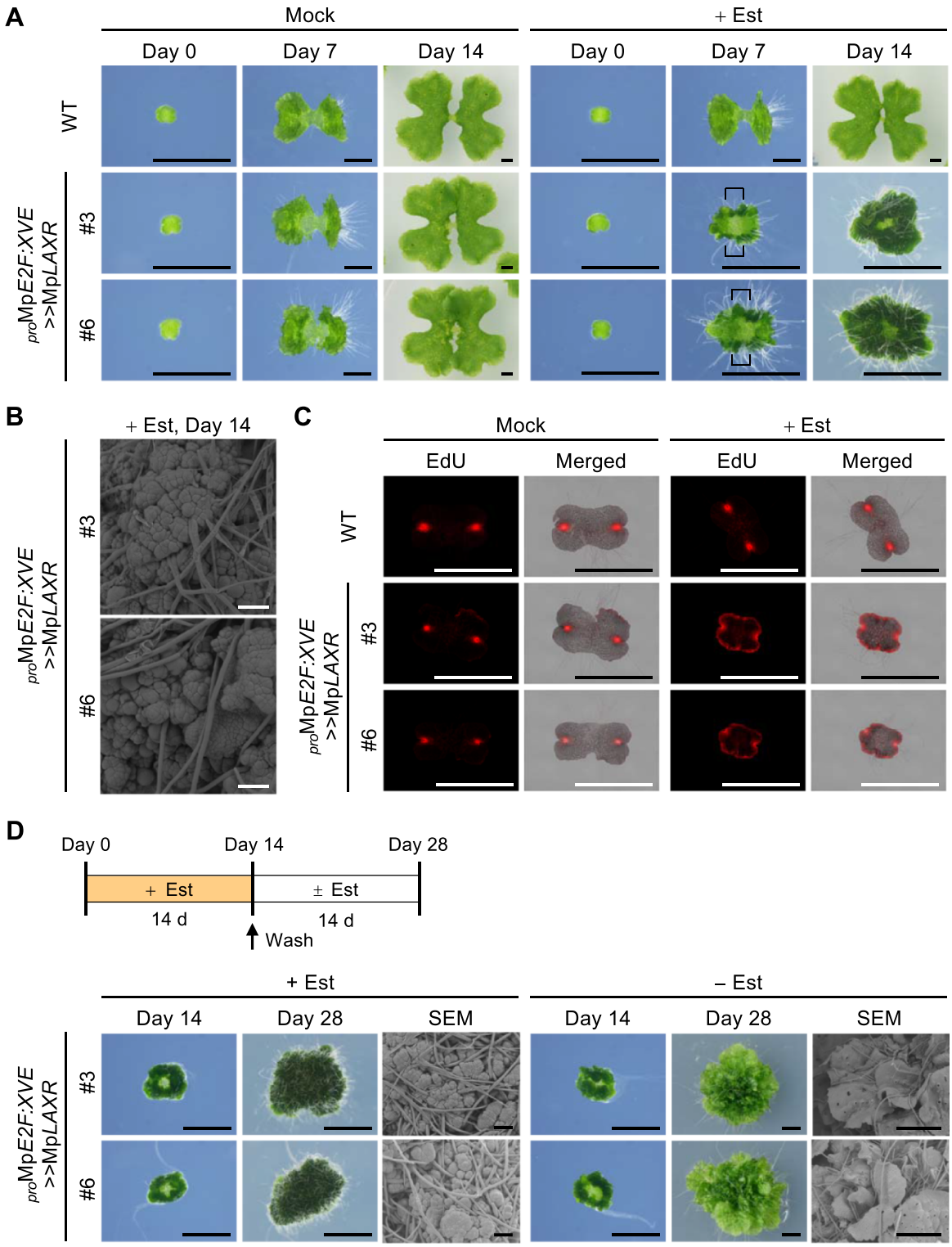

Fig. 9 Function of Mp*LAXR* as a cellular reprogramming factor for thallus regeneration. (A) Images of WT and $_{pro}$Mp*E2F:XVE*≫Mp*LAXR* (lines 3 and 6) gemmalings cultured with or without 5 μM Est for 7 and 14 days. Note that cell masses are formed in regions where cells do not usually divide (brackets). (B) Scanning electron microscope (SEM) images of $_{pro}$Mp*E2F:XVE*≫Mp*LAXR* gemmalings cultured with 5 μM Est for 14 days. (C) EdU incorporation assay of Mp*LAXR*-overexpressing plants. WT and $_{pro}$Mp*E2F:XVE*≫Mp*LAXR* gemmae were cultured with or without 5 μM Est for 3 days and subjected to EdU incorporation assay. Alexa Fluor 555 fluorescence images are shown without or with superimposition on bright field images (merged). (D) Images of $_{pro}$Mp*E2F:XVE*≫Mp*LAXR* plants that were cultured with 5 μM Est for 14 days, washed to remove Est and then further cultured with or without 5 μM Est for 14 days (day 28), as shown in the schematic diagram. Plants at day 28 were also observed under a SEM. Scale bars = 2 mm (A, C and D photographs), 100 μm (B, D SEM images of + Est), 1 mm (D SEM images of – Est).

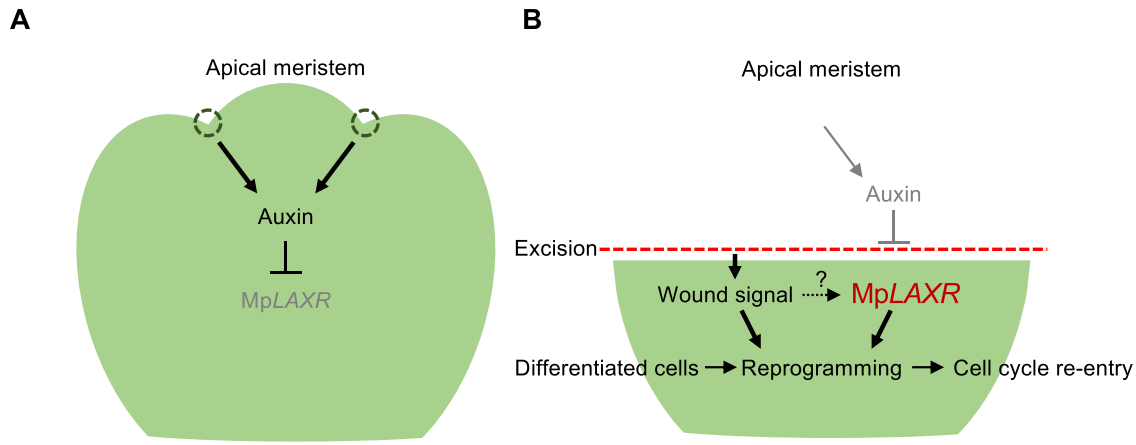

Fig. 10 Regulatory pathways for thallus regeneration in *M. polymorpha*. (A) In intact thalli, auxin is synthesized in the apical meristem and transported to the basal area, where Mp*LAXR* expression is repressed via auxin signaling. (B) Apex amputation, i.e. decapitation, not only generates wound stimuli but also causes transient reduction of auxin levels in the cut surface of basal explants. Lowered auxin signaling induces Mp*LAXR* expression, which triggers reprogramming in concert with the wound signaling pathway.

that are actively dividing at 2–3 days after excision in basal explants (Nishihama et al. 2015). Removal of estrogen allowed thallus development from the cell masses (**Fig. 9D**). These results suggest that overexpression of Mp*LAXR* induces cellular reprogramming to generate undifferentiated cells having the potential for apical stem cell formation.

Discussion

The present data reveal that thallus regeneration in *M. polymorpha* is triggered by a reduction of auxin levels, which induces the cellular reprogramming factor Mp*LAXR* in the meristem-decapitated cut surface to generate undifferentiated cell masses that are competent for stem cell formation toward organized development of regenerating thalli (**Fig. 10**). Down- or up-regulation of Mp*LAXR* by treatment with NAA or its biosynthesis inhibitors, respectively (**Fig. 5**), strongly suggests a negative effect of auxin on Mp*LAXR* expression. This is in line with the observation in Arabidopsis that ARF5/MONOPTEROS-mediated auxin signaling represses *ESR1*/*DRN* at the shoot apex (Luo et al. 2018). Given the short (of the order of minutes) half-lives of AUX/IAA proteins (Abel et al. 1994), reduction of auxin levels over a period of hours should be sufficient for provoking transcriptional responses for Mp*LAXR* induction. A plausible scenario is that in intact thalli, Mp*LAXR* expression is repressed by an auxin-responsive transcriptional repressor and that, upon decapitation, diminished auxin signaling down-regulates the repressor and therefore leads to expression of Mp*LAXR*.

The lack of Mp*LAXR* induction in the apical cut surface (**Fig. 5B** and **Supplementary Fig. S6**) likely indicates no response of Mp*LAXR* to wounding, although the residual Mp*LAXR* induction in NAA-treated basal explants may partly reflect its wound-induced nature, which will require further investigation. The observation that regeneration was delayed but eventually achieved in Mp*laxr* mutants (**Fig. 6C, D**) suggests the existence of a parallel pathway for cellular reprogramming. Among the 30 *M. polymorpha* AP2/ERF genes, which include homologs of class-I *WIND1* (Mp*ERF2*/Mp7g13760) and of class-X *ERF109*, *ERF115*, and *ERF113*/*RAP2.6L* (Mp*ERF9*/Mp4g17430, Mp*ERF21*/Mp5g22160, and Mp*ERF22*/Mp6g11770) but not of STEMIN1 (Bowman et al. 2017, Ishikawa et al. 2019), some showed apparent wound-induced expression (**Supplementary Fig. S6**). These, as well as other wound-induced non-AP2/ERF factors, may cooperate with Mp*LAXR* to regulate cellular reprogramming (**Fig. 10**).

In Arabidopsis, wounding induces the expression of *ESR1*/*DRN* downstream of WIND1, directly and also via cytokinin signaling (Banno et al. 2001, Iwase et al. 2017). However, our hormonal quantification for cytokinins revealed a reduction of *cis*-zeatin, the major cytokinin species in *M. polymorpha* (Aki et al. 2019), and its precursor, *cis*-zeatin riboside phosphates, in basal explants (**Supplementary Fig. S7A**), and therefore the involvement of cytokinin in Mp*LAXR* induction is unclear. RNA-seq and qRT-PCR analyses showed up-regulation of Mp*LOG* and Mp*CKX1*, orthologs of the cytokinin-producing enzyme gene *LONELY GUY* (*LOG*) (Kurakawa et al. 2007) and the cytokinin-inactivating cytokinin oxidase (CKX) gene (Schmülling et al. 2003) respectively, and their suppression by auxin, in basal explants (**Supplementary Fig. S7B, C**). Thus, although cytokinin metabolism may be accelerated in basal explants, it remains under the control of auxin. These data support the notion that the primary trigger of Mp*LAXR* induction in basal explants is the reduced auxin level.

It is currently unclear how auxin level is lowered upon decapitation. Our qRT-PCR data showed temporary down-regulation of Mp*TAA*, but not Mp*YUC2*, at 3 HAE in basal explants (**Supplementary Fig. S8**), which may contribute to the transient reduction of auxin levels to some extent. However, this cannot be the sole explanation because both genes were also

down-regulated in apical explants (**Supplementary Fig. S8**). Inactivation of auxin by chemical modification and/or export of auxin by efflux transporters may be involved in lowering auxin level in the apical side of basal explants. Regarding the polarity of explants, it is also intriguing to point out that thallus regeneration occurs only from the apical side, but not any other sides, of basal explants (this study; Nishihama et al. 2015). The observation that ectopic induction of Mp*LAXR* initiated regeneration also from nonapical sides (**Supplementary Fig. S5**) suggests that the polarity of regeneration is attributable to the restriction of Mp*LAXR* induction to the apical side (**Fig. 5E**). One possible explanation for this phenomenon would be acropetal transport of sucrose along the thallus of *M. polymorpha* (Rota and Maravolo 1975). We have previously shown that sucrose treatment enhanced cell cycle re-entry in basal explants (Nishihama et al. 2015). Besides auxin, other factors, including sugars, are likely to control the polarity of thallus regeneration.

In *M. polymorpha*, depletion of auxin by knockout of the sole *TAA* gene Mp*TAA* (Eklund et al. 2015) or overexpression of an auxin-conjugating enzyme (Flores-Sandoval et al. 2015), or MpIAA^{mDII}-mediated dominant repression of auxin signaling (Kato et al. 2015), results in a failure to establish or maintain the differentiation status of cells and leads to the formation of cell masses. Although our finding that auxin inhibits cell cycle re-entry implies a negative impact of auxin on cell cycle activation, this appears to be an indirect consequence reflecting the primary role of auxin in maintaining the differentiation status, which is likely to be achieved at least partly by repressing the expression of Mp*LAXR*.

Auxin forms gradients in the body and defines developmental axes (Friml 2003, Leyser 2005). Auxin-mediated differential responses between the two surfaces of bisected *M. polymorpha* thalli resemble those in Arabidopsis inflorescence stems for tissue reunion (see Introduction; Asahina et al. 2011). These findings provide an evolutionarily common theme in which the integrity of the plant body is sensed by auxin derived from the apical meristem, a system whose perturbation triggers cellular reprogramming.

Our data demonstrate that a basis of Mp*LAXR* expression is the responsiveness to low levels of auxin as well as its diminished signaling, thus providing a molecular explanation for apical dominance in regeneration. Regarding apical dominance in angiosperms, blocking auxin supply from the shoot apex activates pre-formed dormant axillary meristems (Thimann and Skoog 1934). Therefore, thallus regeneration is different in that reduced auxin induces cellular reprogramming of differentiated cells into undifferentiated cells that are competent for stem cell formation. Recent studies have shown that competency of the axillary meristem is established at an auxin minimum created in the leaf axil (Wang et al. 2014a, 2014b) that maintains low-level expression of the meristem regulator *SHOOTMERISTEMLESS* (*STM*); ESR1/DRN then up-regulates *STM* expression for axillary meristem development (Shi et al. 2016, Zhang et al. 2018). The present study provides an insight into the adaptation of the auxin minimum-dependent class-VIIIb AP2/ERF expression mechanism to stem cell regulation and various forms of apical dominance in land plants.

Materials and Methods

Plant materials and growth conditions

The male *M. polymorpha* accession Takaragaike-1 (Tak-1; used as wild type) (Ishizaki et al. 2008) was cultured on half-strength Gamborg's B5 medium (Gamborg et al. 1968) containing 1% agar under 50–60 μmol photons m^{-2} s^{-1} continuous white light from a cold cathode fluorescent lamp (OPT-40C-N-L, Optrom) at 22°C. F1 spores were obtained by crossing the female *M. polymorpha* accession Takaragaike-2 (Ishizaki et al. 2008) and Tak-1.

Cloning and generation of transgenic lines

Oligo DNAs used in this study are listed in **Supplementary Table S2**. To generate promoter reporter lines of Mp*LAXR*, the promoter sequence of Mp*LAXR* was amplified from wild-type genomic DNA with the primer pair MpLAXR_F1/MpLAXR_R1, and cloned into the pENTR/D-TOPO entry vector (Thermo Fisher Scientific) to generate pENTR/D-TOPO_proMpLAXR. The cloned sequence was transferred to pMpGWB116 (Ishizaki et al. 2015) using LR Clonase II (Thermo Fisher Scientific) to generate pMpGWB116_proMpLAXR, which was introduced into F1 sporelings by *Agrobacterium*-mediated transformation (Ishizaki et al. 2008).

To obtain mutant alleles of Mp*LAXR*, the gRNA oligo DNA sets MpLAXR_gRNA1_A/MpLAXR_gRNA1_B and MpLAXR_gRNA2_A/MpLAXR_gRNA2_B were annealed, followed by ligation reactions with BsaI-digested pMpGE_En03 vector (Sugano et al. 2018, Sugano and Nishihama 2018). The resulting constructs were transferred to the pMpGE010 binary vector (Sugano et al. 2018, Sugano and Nishihama 2018) to generate pMpGE010_MpLAXR_gRNA1 and pMpGE010_MpLAXR_ gRNA2, which were introduced into regenerating thalli of Tak-1 via *Agrobacterium* (Kubota et al. 2013). For the isolation of Mp*laxr-1*^{ge} and Mp*laxr-2*^{ge} mutants, the gRNA1- and gRNA2-targeted regions were amplified from genomic DNAs prepared from transformed thalli using the primer pair MpLAXR_pro_F3/MpLAXR_cds_R2. PCR products were directly sequenced with BigDye Terminator v3.1 (Thermo Fisher Scientific).

To obtain complementation lines of Mp*laxr-1*^{ge} mutants, genomic fragments spanning the promoter to the 3′ UTR, with synonymous substitutions that confer resistance to MpLAXR_gRNA1, were amplified. To insert the mutations, overlap extension PCR was performed with the primer set MpLAXR_pro_F2/MpLAXR_3utr_R using two DNA fragments as templates, one that was amplified by PCR from Tak-1 genomic DNA with the primer pair MpLAXR_pro_F2/MpLAXR_gRNA1_resist_R, and the other with the primer pair MpLAXR_gRNA1_resist_F/MpLAXR_3utr_R. The resulting fragment was then introduced into pENTR/D-TOPO, and the 4.3-kb NotI–PmaCI promoter fragment from pENTR/D-TOPO_proMpLAXR was then inserted into NotI and PmaCI sites to generate pENTR/D-TOPO_proMpLAXR:gMpLAXRresist. The cloned sequence was transferred into pMpGWB301 (Ishizaki et al. 2015) by LR reaction to generate pMpGWB301_proMpLAXR:gMpLAXRresist, which was introduced into Mp*laxr-1*^{ge} plants using regenerating thalli (Kubota et al. 2013).

To obtain the inducible overexpression lines $_{pro}$Mp*E2F:XVE*≫Mp*LAXR*, the CDS of Mp*LAXR* was amplified from Tak-1 genomic DNA with the primer pair MpLAXR_cds_F1/MpLAXR_cds_R and cloned into pENTR/D-TOPO to generate pENTR/D-TOPO_MpLAXR_cds. The cloned sequence was then transferred to pMpGWB168 (details will be published elsewhere) to generate pMpGWB168_MpLAXR, which was introduced into Tak-1 using regenerating thalli (Kubota et al. 2013).

Regeneration assay

Basal and apical explants (prepared as shown in **Fig. 1A**) of wild type, $_{pro}$MpIAA:MpIAA^{mDII}-GR (Kato et al. 2015), $_{pro}$MpLAXR:tdTomato-NLS, Mp*laxr*^{ge}, and $_{pro}$MpLAXR:gMpLAXRresist/Mp*laxr-1*^{ge} were obtained from 10-day-old plants. Explants of Mp*arf1–4*^{ko} (Kato et al. 2017) were obtained from 20-day-old plants due to their slow growth. Explants of $_{pro}$MpE2F:XVE≫MpLAXR plants were obtained from 10-day-old plants after pre-treatment with 5 μM Est for 8 h. Thalli were cut off with a scalpel on a plastic petri dish. Explants were incubated under the standard growth condition described above. For auxin application, explants were transferred onto solid medium with 1 μM NAA and cultured. For the experiment using the $_{pro}$MpIAA:MpIAA^{mDII}-GR line, explants were transferred onto solid medium with or without 1 μM NAA, in the presence or absence of 10 μM Dex, and cultured. Micrographs were captured using an SZX16 stereoscope (Olympus) equipped with a DP20 cooled charge-coupled device. Photographs of the grown thallus were taken with an EOS Kiss X3 digital camera (Canon).

Visualization of S-phase cells

S-phase cells were visualized using a Click-iT EdU Imaging Kit (Thermo Fisher Scientific) according to the manufacturer's instruction and a method described previously (Nishihama et al. 2015). Basal explants of 10-day-old Tak-1 thalli were incubated on solid medium with or without 1 μM NAA under the standard growth condition. At various time points, explants were transferred to a microplate containing half-strength Gamborg's B5 liquid medium with 20 μM EdU, with or without 1 μM NAA, and incubated for 8 h under the same condition. For EdU assay on wild type, Mp*laxr-1*^{ge}, and Mp*laxr-2*^{ge}, explants were incubated with 20 μM EdU for 8 h at various time points. For EdU assay on $_{pro}$MpE2F:XVE≫MpLAXR gemmalings, gemmae were incubated with 20 μM EdU in the presence or absence of 5 μM Est for 24 h after cultivation with or without 5 μM Est on solid medium for 2 days. Incorporation of EdU was terminated by fixing explants with 3.7% formaldehyde solution in phosphate-buffered saline (PBS) for 1 h. After permeabilization with 0.5% Triton X-100 in PBS for 20 min, EdU incorporated into DNA was stained by incubation in the dark with Alexa Fluor 488- or 555-azide-containing Click-iT reaction cocktail for 1 h. After washing successively with PBS containing 3% bovine serum albumin and PBS, DNA was stained with 1 μg ml^{-1} DAPI in PBS overnight in the dark and the explants were washed twice with PBS. Z-series of 10 fluorescence images with 2 μm steps were captured using an all-in-one fluorescence microscope (BZ-X700, Keyence). DAPI and Alexa Fluor 488 and 555 were detected with a filter cube for DAPI, GFP, and TRITC, respectively. GFP fluorescence images were binarized with ImageJ/Fiji (Schindelin et al. 2012, Schneider et al. 2012) and used for measuring EdU-positive areas. Relative EdU-positive areas to whole explant areas were calculated using ImageJ/Fiji.

Quantification of plant hormones

Apical and basal explants were excised from 10-day-old Tak-1 thalli and cultured on half-strength Gamborg's B5 solid medium. One-millimeter sections from the cut surface of the apical and basal explants were sampled at 0, 3, 6, 12, and 24 h. Three biological replicates were prepared for each time point, and 30 sections of the explants (30 to 60 mg fresh weight) were harvested for each replicate. IAA and cytokinin-related compounds were quantified with ultra-high-performance liquid chromatography-quadrupole orbitrap mass spectrometer (UHPLC/Q/Exactive; Thermo Scientific) and ultra-performance liquid chromatography-tandem quadrupole mass spectrometer (ACQUITY UPLC System/XEVO-TQS; Waters), respectively, as described previously (Kojima and Sakakibara 2012, Shinozaki et al. 2015).

Transcriptome analysis

Total RNA was extracted from the 1 mm sections from the cut surface of apical and basal explants of Tak-1 incubated with or without 1 μM NAA for 0, 1, 3, 6, 12, and 24 HAE, using an RNeasy Plant Mini kit (Qiagen). For the samples at 0, 3, 6, and 24 HAE without NAA, sequence libraries were prepared using a TruSeq RNA Sample Prep Kit v.2 (Illumina) and sequenced using Illumina HiSeq 1500 with a 126-nt single-end sequencing protocol. For the samples at 1 HAE with or without NAA, and 3 and 6 HAE with NAA, the sequence libraries were prepared and their sequencing performed by Macrogen Japan using NovaSeq 6000. Three biological replicates were prepared for each time point, and 30 sections of the explants were harvested for each replicate.

Default settings were used for the *in silico* assays below unless otherwise mentioned. The sequence reads were filtered using fastp v0.20.1 (Chen et al. 2018). The cleaned reads were mapped to the *M. polymorpha* genome sequence v.5.1_r1 (MarpolBase, https://marchantia.info; Montgomery et al. 2020) using STAR v2.6.1c (Dobin et al. 2013). The mapped reads were counted using the *featureCounts* function of the Rsubread package v2.2.6 (Liao et al. 2019).

Samples were classified by PCA based on $\log_2$-transformed read counts of all genes using the *rlog* and subsequently *plotPCA* functions of the DESeq2 package v1.28.1 (Love et al. 2014). Fold changes and adjusted *P*-values of genes compared with 0 HAE were calculated by Wald test based on the raw read counts using the *DESeq* function of the DESeq2 package.

Auxin-responsive genes were calculated as described above using public RNA-seq data of 2,4-D-treated thalli (SRR5905091, SRR5905092 and SRR5905097) and their controls (SRR5905098, SRR5905099 and SRR5905100; Mutte et al. 2018), which were downloaded from SRA (https://www.ncbi.nlm.nih.gov/sra). Enrichment of the auxin-responsive genes in excision-up- or -down-regulated genes compared with 0 HAE (adjusted *P*-value < 0.001) was assessed by Fisher's exact test using the *fisher.test* function (R v4.0.0, https://www.R-project.org/).

Genes were classified based on the read counts using clust v1.12.0 (Abu-Jamous and Kelly 2018). GO terms were annotated for the version 5.1_r1 genome of *M. polymorpha* using NetGO v2.0 (You et al. 2019), Argot2 (Falda et al. 2012), PANNZER2 (Törönen et al. 2018) and DeepGOPlus v1.0.1 (Kulmanov and Hoehndorf 2020). The annotations were filtered out with <0.6 score in NetGo, <0.7 score in Argot2, <0.7 PPV score in PANNZER2 and <0.3 score in DeepGOPlus. These four in-house annotations, the annotations from MarpolBase and another one previously reported (Hernández-García et al. 2021) were processed for data merge and duplicate removal and then used to build an annotation database with the AnnotationForge package v1.30.1 (https://bioconductor.org/packages/release/bioc/html/AnnotationForge.html). GO terms enriched in each cluster were detected using the *enrichGO* function of the clusterProfiler package v3.16.1 (Yu et al. 2012). The enriched GO terms were summarized using the *calculateSimMatrix* and, subsequently, *reduceSimMatrix* functions of the rrvgo package v1.0.2 (https://bioconductor.org/packages/release/bioc/html/rrvgo.html) with similarity thresholds 0.85, 0.7 and 0.75 for 'Biological Process,' 'Cellular Component' and 'Molecular Function', respectively.

To depict heatmaps, distances among genes were calculated based on $\log_2$ fold change value using the *dist* function, and clusters were then calculated by the ward.D2 method using the *hclust* function (R v4.0.0).

Quantitative real-time RT-PCR

Total RNA of wild-type, Mp*laxr-1*^{ge} and Mp*laxr-2*^{ge} explants was extracted from cut surface samples harvested as described in **Fig. 2D** using TRIzol reagent (Thermo Fisher Scientific). Total RNA of 10-day-old wild-type and $_{pro}$MpIAA:MpIAA^{mDII}-GR plants treated with or without 10 μM Dex for 12 h was extracted as described above and treated with RNase-Free DNase (Qiagen) following the manufacturer's instructions. Reverse transcription was performed with 0.5–1.0 μg of RNA and an oligo(dT) primer using ReverTraAce (Toyobo) following the manufacturer's instructions. qRT-PCR was performed with a CFX96 real-time PCR detection system (Bio-Rad) using SYBR Green I Nucleic Acid Gel Stain (Lonza) to monitor double-stranded DNA synthesis. Primer pairs used for each gene are shown in **Supplementary Table S2**. The following thermal cycling profile was used for all PCRs: 95°C for 30 s, and 40 cycles of 95°C for

5 s and 60°C for 30 s. Mp*EF1* was used as an internal control for normalization of the PCR.

Auxin biosynthesis inhibitor treatment

Tak-1 gemmae were grown on medium containing 10 μM PPBo (Kakei et al. 2015), 10 μM yucasin (Nishimura et al. 2014) or 100 μM L-kynurenine (He et al. 2011) for 3 days, and total RNA was extracted as described above for quantification of Mp*LAXR* expression levels.

Measurement of projection areas

Thallus or regenerant areas were calculated as projection areas using images captured from the top, which were measured by the Measure tool in ImageJ/Fiji using binary images converted from blue channel images of color photographs. Projection areas of regenerants were calculated by subtracting the measured area of day 0 from that of day 7.

Fluorescence observation

For the visualization of Mp*LAXR* promoter activity during regeneration, Z-series of 10 fluorescence images with 2-μm steps on the ventral surface of basal explants of $_{pro}$Mp*LAXR:tdTomato-NLS* were captured using a BZ-X700 with a filter cube for TRITC and were integrated into a single file using the Full Focus application within the BZ-X700 Analyzer software (Keyence).

Scanning electron microscope observation

Scanning electron microscope images in **Fig. 9** were taken using a TM3000 (Hitachi High Technologies) as described before (Nishihama et al. 2015).

Supplementary Data

Supplementary data are available at *PCP* online.

Data Availability

The nucleotide sequence reported in this article has been submitted to DDBJ 455 at http://ddbj.nig.ac.jp/arsa/ under accession number LC651162. The data underlying this article are available in the DDBJ at https://www.ddbj.nig.ac.jp/dra/ and can be accessed with BioProject number PRJDB12610 (DRX319152–DRX319190). The data used to evaluate the conclusions in this paper are available in NCBI Short Read Archive at https://www.ncbi.nlm.nih.gov/sra and can be accessed with BioProject number PRJNA397394 (SRR5905091, SRR5905092, SRR5905097, SRR5905098, SRR5905099 and SRR5905100; Mutte et al. 2018).

Funding

This work was supported by JSPS KAKENHI (JP18J12698 to H.Su.; JP25113001, JP17H07424, and JP19H05675 to T.K.; JP16K07398 and JP20H04884 to R.N.), NIBB Collaborative Research Program (17-425) to T.K. and SPIRITS 2017 of Kyoto University to R.N.

Acknowledgements

We thank Yoshihiro Yoshitake and Keita Kinose for providing plasmids for estrogen-inducible overexpression, Ken-ichiro Hayashi for providing the auxin biosynthesis inhibitors PPBo and yucasin, Yoriko Matsuda for experimental support, Keisuke Inoue for experimental support and discussion, Ian Smith for critically editing the manuscript, and two anonymous reviewers for helpful comments on the manuscript.

Author Contributions

S.I., T.K. and R.N. conceived and designed the research. S.I. and A.I. performed the experiments. M.K., Y.T. and H.Sa. performed the hormone quantification experiments. H.Su., S.K., S.Y., K.Y. and S.S. performed and contributed to the RNA-seq experiments. S.I., H.Su., T.K. and R.N. analyzed the data. S.I., H.Su. and R.N. wrote the manuscript. All authors reviewed and edited the manuscript.

Disclosures

No conflicts of interest declared.

References

Abel, S., Oeller, P.W. and Theologis, A. (1994) Early auxin-induced genes encode short-lived nuclear proteins. *Proc. Natl. Acad. Sci. U.S.A.* 91: 326–330.

Abu-Jamous, B. and Kelly, S. (2018) Clust: automatic extraction of optimal co-expressed gene clusters from gene expression data. *Genome Biol.* 19: 172.

Aki, S.S., Mikami, T., Naramoto, S., Nishihama, R., Ishizaki, K., Kojima, M., et al. (2019) Cytokinin signaling is essential for organ formation in *Marchantia polymorpha*. *Plant Cell Physiol.* 60: 1842–1854.

Asahina, M., Azuma, K., Pitaksaringkarn, W., Yamazaki, T., Mitsuda, N., Ohme-Takagi, M., et al. (2011) Spatially selective hormonal control of RAP2.6L and ANAC071 transcription factors involved in tissue reunion in *Arabidopsis*. *Proc. Natl. Acad. Sci. USA.* 108: 16128–16132.

Banno, H., Ikeda, Y., Niu, Q.W. and Chua, N.H. (2001) Overexpression of Arabidopsis *ESR1* induces initiation of shoot regeneration. *Plant Cell* 13: 2609–2618.

Bowman, J.L., Kohchi, T., Yamato, K.T., Jenkins, J., Shu, S., Ishizaki, K., et al. (2017) Insights into land plant evolution garnered from the *Marchantia polymorpha* genome. *Cell* 171: 287–304.e15.

Chandler, J.W. (2018) Class VIIIb APETALA2 ethylene response factors in plant development. *Trends Plant Sci.* 23: 151–162.

Chen, L., Tong, J., Xiao, L., Ruan, Y., Liu, J., Zeng, M., et al. (2016) YUCCA-mediated auxin biogenesis is required for cell fate transition occurring during de novo root organogenesis in Arabidopsis. *J. Exp. Bot.* 67: 4273–4284.

Chen, S., Zhou, Y., Chen, Y. and Gu, J. (2018) fastp: an ultra-fast all-in-one FASTQ preprocessor. *Bioinformatics* 34: i884–i890.

Dobin, A., Davis, C.A., Schlesinger, F., Drenkow, J., Zaleski, C., Jha, S., et al. (2013) STAR: ultrafast universal RNA-seq aligner. *Bioinformatics* 29: 15–21.

Efroni, I., Mello, A., Nawy, T., Ip, P.L., Rahni, R., Delrose, N., et al. (2016) Root regeneration triggers an embryo-like sequence guided by hormonal interactions. *Cell* 165: 1721–1733.

Eklund, D.M., Ishizaki, K., Flores-Sandoval, E., Kikuchi, S., Takebayashi, Y., Tsukamoto, S., et al. (2015) Auxin produced by the indole-3-pyruvic acid pathway regulates development and gemmae dormancy in the liverwort *Marchantia polymorpha*. *Plant Cell* 27: 1650–1669.

Falda, M., Toppo, S., Pescarolo, A., Lavezzo, E., Di Camillo, B., Facchinetti, A., et al. (2012) Argot2: a large scale function prediction tool relying on

semantic similarity of weighted gene ontology terms. *BMC Bioinform.* 13 Suppl 4: S14.

Flores-Sandoval, E., Eklund, D.M. and Bowman, J.L. (2015) A simple auxin transcriptional response system regulates multiple morphogenetic processes in the liverwort *Marchantia polymorpha*. *PLoS Genet.* 11: 1–26.

Friml, J. (2003) Auxin transport - shaping the plant. *Curr. Opin. Plant Biol.* 6: 7–12.

Gaal, D.J., Dufresne, S.J. and Maravolo, N.C. (1982) Transport of ^{14}C-indoleacetic acid in the hepatic *Marchantia polymorpha*. *Bryologist* 85: 410–418.

Gamborg, O.L., Miller, R.A. and Ojima, K. (1968) Nutrient requirements of suspension cultures of soybean root cells. *Exp. Cell Res.* 50: 151–158.

He, W., Brumos, J., Li, H., Ji, Y., Ke, M., Gong, X., et al. (2011) A small-molecule screen identifies L-Kynurenine as a competitive inhibitor of TAA1/TAR activity in ethylene-directed auxin biosynthesis and root growth in *Arabidopsis*. *Plant Cell.* 23: 3944–3960.

Hernández-García, J., Sun, R., Serrano-Mislata, A., Inoue, K., Vargas-Chávez, C., Esteve-Bruna, D., et al. (2021) Coordination between growth and stress responses by DELLA in the liverwort *Marchantia polymorpha*. *Curr. Biol.* 31: 3678–3686.e11.

Ishikawa, M., Morishita, M., Higuchi, Y., Ichikawa, S., Ishikawa, T., Nishiyama, T., et al. (2019) Physcomitrella STEMIN transcription factor induces stem cell formation with epigenetic reprogramming. *Nat. Plants* 5: 681–690.

Ishikawa, M., Murata, T., Sato, Y., Nishiyama, T., Hiwatashi, Y., Imai, A., et al. (2011) Physcomitrella cyclin-dependent kinase a links cell cycle reactivation to other cellular changes during reprogramming of leaf cells. *Plant Cell* 23: 2924–2938.

Ishizaki, K., Chiyoda, S., Yamato, K.T. and Kohchi, T. (2008) *Agrobacterium*-mediated transformation of the haploid liverwort *Marchantia polymorpha* L., an emerging model for plant biology. *Plant Cell Physiol.* 49: 1084–1091.

Ishizaki, K., Nishihama, R., Ueda, M., Inoue, K., Ishida, S., Nishimura, Y., et al. (2015) Development of gateway binary vector series with four different selection markers for the liverwort *Marchantia polymorpha*. *PLoS One* 10: e0138876.

Iwase, A., Harashima, H., Ikeuchi, M., Rymen, B., Ohnuma, M., Komaki, S., et al. (2017) WIND1 promotes shoot regeneration through transcriptional activation of *ENHANCER OF SHOOT REGENERATION1* in Arabidopsis. *Plant Cell* 29: 54–69.

Iwase, A., Mitsuda, N., Koyama, T., Hiratsu, K., Kojima, M., Arai, T., et al. (2011) The AP2/ERF transcription factor WIND1 controls cell dedifferentiation in *Arabidopsis*. *Curr. Biol.* 21: 508–514.

Kakei, Y., Yamazaki, C., Suzuki, M., Nakamura, A., Sato, A., Ishida, Y., et al. (2015) Small-molecule auxin inhibitors that target YUCCA are powerful tools for studying auxin function. *Plant J.* 84: 827–837.

Kato, H., Ishizaki, K., Kouno, M., Shirakawa, M., Bowman, J.L., Nishihama, R., et al. (2015) Auxin-mediated transcriptional system with a minimal set of components is critical for morphogenesis through the life cycle in *Marchantia polymorpha*. *PLoS Genet.* 11: e1005365.

Kato, H., Kouno, M., Takeda, M., Suzuki, H., Ishizaki, K., Nishihama, R., et al. (2017) The roles of the sole activator-type auxin response factor in pattern formation of *Marchantia polymorpha*. *Plant Cell Physiol.* 58: 1642–1651.

Kato, H., Mutte, S.K., Suzuki, H., Crespo, I., Das, S., Radoeva, T., et al. (2020) Design principles of a minimal auxin response system. *Nat. Plants* 6: 473–482.

Kohchi, T., Yamato, K.T., Ishizaki, K., Yamaoka, S. and Nishihama, R. (2021) Development and molecular genetics of *Marchantia polymorpha*. *Annu. Rev. Plant Biol.* 72: 677–702.

Kojima, M. and Sakakibara, H. (2012) Highly sensitive high-throughput profiling of six phytohormones using MS-probe modification and liquid chromatography–tandem mass spectrometry. *Methods Mol. Biol.* 918: 151–164.

Kubota, A., Ishizaki, K., Hosaka, M. and Kohchi, T. (2013) Efficient *Agrobacterium*-mediated transformation of the liverwort *Marchantia polymorpha* using regenerating thalli. *Biosci. Biotechnol. Biochem.* 77: 167–172.

Kulmanov, M. and Hoehndorf, R. (2020) DeepGOPlus: improved protein function prediction from sequence. *Bioinformatics* 36: 422–429.

Kurakawa, T., Ueda, N., Maekawa, M., Kobayashi, K., Kojima, M., Nagato, Y., et al. (2007) Direct control of shoot meristem activity by a cytokinin-activating enzyme. *Nature* 445: 652–655.

LaRue, C. and Narayanaswami, S. (1957) Auxin inhibition in the liverwort *Lunularia*. *New Phytol.* 56: 61–70.

Leyser, O. (2005) Auxin distribution and plant pattern formation: how many angels can dance on the point of PIN? *Cell* 121: 819–822.

Liao, Y., Smyth, G.K. and Shi, W. (2019) The R package *Rsubreadis* easier, faster, cheaper and better for alignment and quantification of RNA sequencing reads. *Nucleic Acids Res.* 47: e47.

Love, M.I., Huber, W. and Anders, S. (2014) Moderated estimation of fold change and dispersion for RNA-seq data with DESeq2. *Genome Biol.* 15: 550.

Luo, L., Zeng, J., Wu, H., Tian, Z. and Zhao, Z. (2018) A molecular framework for auxin-controlled homeostasis of shoot stem cells in *Arabidopsis*. *Mol. Plant* 11: 899–913.

Masubelele, N.H., Dewitte, W., Menges, M., Maughan, S., Collins, C., Huntley, R., et al. (2005) D-type cyclins activate division in the root apex to promote seed germination in Arabidopsis. *Proc. Natl. Acad. Sci. U.S.A.* 102: 15694–15699.

Montgomery, S.A., Tanizawa, Y., Galik, B., Wang, N., Ito, T., Mochizuki, T., et al. (2020) Chromatin organization in early land plants reveals an ancestral association between H3K27me3, transposons, and constitutive heterochromatin. *Curr. Biol.* 30: 573–588.e7.

Mutte, S.K., Kato, H., Rothfels, C., Melkonian, M., Wong, G.K.S. and Weijers, D. (2018) Origin and evolution of the nuclear auxin response system. *eLife* 7: e33399.

Nishihama, R., Ishizaki, K., Hosaka, M., Matsuda, Y., Kubota, A. and Kohchi, T. (2015) Phytochrome-mediated regulation of cell division and growth during regeneration and sporeling development in the liverwort *Marchantia polymorpha*. *J. Plant Res.* 128: 407–421.

Nishimura, T., Hayashi, K.I., Suzuki, H., Gyohda, A., Takaoka, C., Sakaguchi, Y., et al. (2014) Yucasin is a potent inhibitor of YUCCA, a key enzyme in auxin biosynthesis. *Plant J.* 77: 352–366.

Powers, S.K. and Strader, L.C. (2020) Regulation of auxin transcriptional responses. *Dev. Dyn.* 249: 483–495.

Rota, J. and Maravolo, N.C. (1975) Transport and mobilization of ^{14}C-sucrose during regeneration in the hepatic, *Marchantia polymorpha*. *Bot. Gaz.* 136: 184–188.

Schindelin, J., Arganda-Carrera, I., Frise, E., Verena, K., Mark, L., Tobias, P., et al. (2012) Fiji - an open source platform for biological image analysis. *Nat. Methods* 9: 676–682.

Schmülling, T., Werner, T., Riefler, M., Krupková, E., Bartrina, Y. and Manns, I. (2003) Structure and function of cytokinin oxidase/dehydrogenase genes of maize, rice, Arabidopsis and other species. *J. Plant Res.* 116: 241–252.

Schneider, C.A., Rasband, W.S. and Eliceiri, K.W. (2012) NIH Image to ImageJ: 25 years of image analysis. *Nat. Methods* 9: 671–675.

Shi, B., Zhang, C., Tian, C., Wang, J., Wang, Q., Xu, T., et al. (2016) Two-step regulation of a meristematic cell population acting in shoot branching in *Arabidopsis*. *PLoS Genet.* 12: e1006168.

Shinozaki, Y., Hao, S., Kojima, M., Sakakibara, H., Ozeki-Iida, Y., Zheng, Y., et al. (2015) Ethylene suppresses tomato (*Solanum lycopersicum*) fruit set through modification of gibberellin metabolism. *Plant J.* 83: 237–251.

Sugano, S.S. and Nishihama, R. (2018) CRISPR/Cas9-based genome editing of transcription factor genes in *Marchantia polymorpha*. *Methods Mol. Biol.* 1830: 109–126.

Sugano, S.S., Nishihama, R., Shirakawa, M., Takagi, J., Matsuda, Y., Ishida, S., et al. (2018) Efficient CRISPR/Cas9-based genome editing and its application to conditional genetic analysis in *Marchantia polymorpha*. *PLoS One* 13: e0205117.

Thimann, K.V. and Skoog, F. (1934) On the inhibition of bud development and other functions of growth substance in *Vicia faba*. *Proc. Royal Soc. B* 114: 317–339.

Törönen, P., Medlar, A. and Holm, L. (2018) PANNZER2: a rapid functional annotation web server. *Nucleic Acids Res.* 46: W84–W88.

Umeda, M., Ikeuchi, M., Ishikawa, M., Ito, T., Nishihama, R., Kyozuka, J., et al. (2021) Plant stem cell research is uncovering the secrets of longevity and persistent growth. *Plant J.* 106: 326–335.

Vöchting, H. (1885) Ueber die regeneration der Marchantieen. *Jahrbücher Für Wissenschaftliche Bot.* 16: 367–414.

Wang, Q., Kohlen, W., Rossmann, S., Vernoux, T. and Theres, K. (2014a) Auxin depletion from the leaf axil conditions competence for axillary meristem formation in *Arabidopsis* and tomato. *Plant Cell* 26: 2068–2079.

Wang, Y., Wang, J., Shi, B., Yu, T., Qi, J., Meyerowitz, E.M., et al. (2014b) The stem cell niche in leaf axils is established by auxin and cytokinin in *Arabidopsis*. *Plant Cell* 26: 2055–2067.

Weijers, D. and Wagner, D. (2016) Transcriptional responses to the auxin hormone. *Annu. Rev. Plant Biol.* 67: 539–574.

You, R., Yao, S., Xiong, Y., Huang, X., Sun, F., Mamitsuka, H., et al. (2019) NetGO: improving large-scale protein function prediction with massive network information. *Nucleic Acids Res.* 47: W379–W387.

Yu, G., Wang, L.G., Han, Y. and He, Q.Y. (2012) ClusterProfiler: an R package for comparing biological themes among gene clusters. *OMICS* 16: 284–287.

Zhang, C., Wang, J., Wenkel, S., Chandler, J.W., Werr, W. and Jiao, Y. (2018) Spatiotemporal control of axillary meristem formation by interacting transcriptional regulators. *Development* 145: dev158352.

Zhang, G., Zhao, F., Chen, L., Pan, Y., Sun, L., Bao, N., et al. (2019) Jasmonate-mediated wound signalling promotes plant regeneration. *Nat. Plants* 5: 491–497.

Zhou, W., Lozano-Torres, J.L., Blilou, I., Zhang, X., Zhai, Q., Smant, G., et al. (2019) A jasmonate signaling network activates root stem cells and promotes regeneration. *Cell* 177: 942–956.e14.